Dimerization Is Crucial for the Function of the Na^+/H^+ Exchanger NHE1[†]

Takashi Hisamitsu, Youssef Ben Ammar, Tomoe Y. Nakamura, and Shigeo Wakabayashi*

Department of Molecular Physiology, National Cardiovascular Center Research Institute, Suita, Osaka 565-8565, Japan

Received May 2, 2006; Revised Manuscript Received August 15, 2006

ABSTRACT: The Na^+/H^+ exchanger 1 (NHE1) exists as a homo-dimer in the plasma membranes. In the present study, we have investigated the functional significance of the dimerization, using two nonfunctional NHE1 mutants, surface-expression-deficient G309V and transport-deficient E262I. Biochemical and immunocytochemical experiments revealed that these NHE1 mutants are capable of interacting with the wild-type NHE1 and, thus, forming a heterodimer. Expression of G309V retained the wild-type NHE1 to the ER membranes, suggesting that NHE1 would first form a dimer in the ER. On the other hand, expression of E262I markedly reduced the exchange activity of the wild-type NHE1 through an acidic shift in the intracellular pH (pH_i) dependence, suggesting that dimerization is required for exchange activity in the physiological pH_i range. However, a dominant−negative effect of E262I was not detected when exchange activity was measured at acidic pH_i, implying that one active subunit is sufficient to catalyze ion transport when the intracellular H^+ concentration is sufficiently high. Furthermore, intermolecular cysteine cross-linking at extracellular position Ser^{375} with a bifunctional sulfhydryl reagent dramatically inhibited exchange activity mainly by inducing the acidic shift of pH_i dependence and abolished extracellular stimuli-induced activation of NHE1 without causing a large change in the affinities for extracellular Na^+ or an inhibitor EIPA. Because monofunctional sulfhydryl regents had no effect, it is likely that cross-linking inhibited the activity of NHE1 by restricting a coupled motion between the two subunits during transport. Taken together, these data support the view that dimerization of two active subunits are required for NHE1 to possess the exchange activity in the neutral pH_i range, although each subunit is capable of catalyzing transport in the acidic pH_i range.

The Na^+/H^+ exchanger (NHE[1]) is a member of the secondary active transporter family, which catalyzes the exchange of Na^+ for H^+ (*1*−*5*). NHE isoforms (NHE1−NHE9) possess a common structural feature, that is, the molecules have two large functional domains, an amino (*N*-) terminal membrane domain consisting of multiple membrane-spanning helices and a long carboxyl (*C*-) terminal hydrophilic domain. Of nine known isoforms, NHE1 is ubiquitously expressed and is responsible for the control of intracellular pH (pH_i) and cell volume (*1*−*5*). NHE1 is known to be activated in response to various extrinsic stimuli such as hormones, growth factors, and changes in the medium osmolarity, presumably through the interaction of various signaling molecules with the *C*-terminal cytoplasmic domain. Importantly, such activation of NHE1 is thought to be exerted through a conformational change of the exchanger molecule, which is triggered by protonation at a H^+-modifier or pH sensor site that is distinct from the H^+-transport site (*6*−*8*).

In contrast to the extensive studies investigating the regulatory mechanism of NHE1, structural information including the subunit-subunit interaction is extremely limited. A previous study showed that NHE1 and NHE3 form homo-oligomers by interacting via the transmembrane regions in intact cells (*9*), and consistent with this, NHE1 in the placental brush border membranes was detected as a larger form (∼205 kDa), cross-linked by disulfide bonds (*10*). Furthermore, we recently presented evidence that NHE1 forms a homodimer but not a homotrimer or a homotetramer (*11*). Despite detailed descriptions of the oligomeric state of the exchanger, its functional significance is not well understood. The previous study (*9*) suggested that the functional unit of NHE1 is a monomer on the basis of the coexpression experiment of transport-deficient mutant E262I. However, it has been reported that the interaction between

[†] This work was supported by a Grant-in-Aid for Priority Areas 13142210 for Scientific Research from the Ministry of Education, Science Culture of Japan, by Grant nano-001 for Research on Advanced Medical Technology from the Ministry of Health, Labor, and Welfare of Japan, and by the Program for Promotion of Fundamental Studies in Health Science of the National Institute of Biomedical Innovation (NIBIO).

* To whom correspondence should be addressed. Tel: 81-6-6833-5012. Fax: 81-6-6835-5314. E-mail: wak@ri.ncvc.go.jp.

[1] Abbreviations: NHE, Na^+/H^+ exchanger; pH_i, intracellular pH; EL, extracellular loop; IL, intracellular loop; TM, transmembrane spanning region; ER, endoplasmic reticulum; MTS-2, 1,2-ethanediyl-bis-methanethiosulfonate; MTS-6, 1,6-hexanediyl-bis-methanethiosulfonate; MTS-17, 3,6,9,12,15,-pentaoxaheptadecane-1,17-diyl-bis-methanethiosulfonate; MTSET, 2-(trimethylammonium) ethyl methanethiosulfonate; PMA, phorbol 12-myristate 13-acetate; EIPA, 5-(*N*-ethyl-*N*-isopropyl)amiloride; NHS-LC-biotin, succinimidyl-6-(biotinamide)-hexanoate; $DiOC_6(3)$, 3,3′-dihexyloxacarbocyanine iodide; BCECF-AM, 2′,7′-bis-(2-carboxyethyl)-5(6)-carboxyfluorescein acetoxymethyl ester; HA, hemaglutinin; PCR, polymerase chain reaction; DMEM, Dulbecco's modified Eagle's medium; HEPES, 2-[4-(2-hydroxyethyl)-1-piperazinyl]ethanesulfonic acid; Tris, Tris(hydroxymethyl)aminomethane; EDTA, ethylenediamine-*N*,*N*,*N*′,*N*′-tetraacetic acid; PBS, phosphate-buffered saline; PAGE, polyacrylamide gel electrophoresis; SH, sulfhydryl; LDS, lithium dodecylsulfate; CCD, charge coupled device; aa, amino acid.

10.1021/bi0608616 CCC: $33.50
Published on Web 10/17/2006

subunits may be required for NHE1 function using several kinetic approaches (*12*−*14*). In addition, the sigmoidal cytosolic H^+ dependence has recently been reported to be best explained by an allosteric model involving the cooperative interaction between subunits (*14*).

In this study, we have addressed whether dimerization is responsible for the activity of NHE1. We found that expression of a dominant-negative mutant exchanger greatly inhibited the exchange activity in the neutral pH_i range by inducing an acidic shift of the pH_i dependence. Furthermore, the exchange activity was markedly reduced by intermolecular cross-linking between engineered cysteine residues, suggesting that cross-linking restricts the cooperative movement between NHE1 subunits and thereby inhibits ion transport. The present findings provide a strong piece of evidence that dimerization is required for the physiological function of NHE1.

EXPERIMENTAL PROCEDURES

Antibodies and Other Materials. The polyclonal antibody against human NHE1 has been described previously (*15*). Antibodies against HA (3F10) and c-Myc epitopes were purchased from Roche Diagnostics GmbH (Germany) and Santa Cruz Biotechnology, Inc. (CA), respectively. Cysteine-modifier reagent MTSET and cross-linkers MTS-2, MTS-6, and MTS-17 were purchased from Toronto Research Chemicals, Inc. (Canada). ^{22}NaCl and [^{14}C]-benzoic acid were purchased from Perkin-Elmer Life Science, Inc. (MA). All other chemicals were of the highest purity available.

Cell Culture and Plasmid DNA Transfection. The exchanger-deficient cell line (PS120) (*16*) and corresponding transfectants were maintained in DMEM containing 25 mM $NaHCO_3$ and supplemented with 7.5% (v/v) fetal calf serum, penicillin (50 units/mL), and streptomycin (50 μg/mL). Cells were maintained at 37 °C in the presence of 5% CO_2. All cDNA constructs were transfected into PS120 or CCL39 cells using the calcium phosphate-DNA coprecipitation technique or with Lipofectamine 2000 (Invitrogen Corp., CA), and stable clones for NHE1 and mutant constructs were selected by repetitive H^+-killing selection procedures, as described previously (*17*). In some cases, G418-resistant cell clones were isolated.

Construction of the NHE1 Mutant Plasmid. A plasmid carrying a cDNA encoding human NHE1 and containing unique restriction sites cloned into the mammalian expression vector pECE has been described previously (*17*). A cDNA construct for NHE1 in which all endogenous cysteine residues were replaced by alanine, designated as Cys-less NHE1, has also been described previously (*18*). Construction of plasmids for NHE1 containing point mutations was carried out by a PCR-based strategy using two template plasmids encoding wild-type or Cys-less NHE1, as described previously (*18*). Similarly, plasmids containing nucleotide sequences corresponding to the HA epitope YPYDVPDYAS or the c-Myc epitope EQKLISEEDL were constructed by inserting PCR fragments produced using antisense primers containing either epitope sequence and a stop codon just after the *C*-terminus of NHE1 into the appropriate restriction sites of the plasmid containing NHE1 cDNA. Constructs were confirmed by sequencing plasmids with an ABI-PRISM DNA sequencer model 3100 (Applied Biosystems, CA). In this study, we use the prefix "cl-" for point mutants produced from Cys-less NHE1 as background.

Cross-Linking between Cysteine Residues of NHE1. The cross-linking reaction was performed using PS120 cells stably expressing the NHE1 mutants, essentially as described previously (*11*). Cells expressing each mutant containing a single cysteine residue at an extracellular site of Cys-less NHE1 were grown to confluence, usually on a 12-well plate, and then were washed twice with balanced salt solution (BSS) containing 136 mM NaCl, 4 mM KCl, 1 mM $MgCl_2$, 1.8 mM $CaCl_2$, 5 mM glucose, and 10 mM HEPES at pH 7.4 adjusted with NaOH. Cells were then treated with various thiol-specific cross-linkers, MTS-2, MTS-6, and MTS-17 (usually 0.1−1.0 mM), in the above solution for 15 min at room temperature. The cross-linking reaction was stopped by the addition of 300 μL of 2× LDS sample buffer (Invitrogen) containing 10 mM *N*-ethylmaleimide per well, and then the PAGE mobility of NHE1 variants in the samples was analyzed by immunoblotting.

Immunoprecipitation and Immunoblotting. For co-immunoprecipitation of the Myc-tagged wild-type NHE1 and the HA-tagged E262I mutant, cells coexpressing these proteins were washed with ice-cold PBS and solubilized with lysis buffer (1% Triton X-100, 5 mM EDTA, 1 mM phenylmethylsulfonyl fluoride, and 1 mM benzamidine in PBS) for 20 min on ice. Quantitative analysis revealed that most of NHE1 (88 ± 4%) was recovered in the Triton-soluble fraction. After centrifugation for 5 min at 15,000 rpm, the supernatant (Triton-soluble fraction) was incubated for 2 h at 4 °C with rabbit anti-Myc antibody plus 30 μL of Protein A-Sepharose beads (Amersham Biosciences, Inc., NJ). The beads were washed five times with ice-cold lysis buffer, and proteins were eluted with LDS sample buffer containing 50 mM DTT. After PAGE on 3−8% gradient gels (NuPAGE Gel, Invitrogen), proteins were transferred electrophoretically onto polyvinylidene difluoride membranes and subjected to immunoblotting with anti-HA. Proteins were visualized by enhanced chemiluminescence detection (Amersham).

Immunocytochemistry. Cells were fixed with cold methanol and then blocked with PBS containing 5% BSA fraction IV. Cells were then treated with anti-NHE1 or anti-HA antibody followed by fluorescent staining with a rhodamine-labeled secondary antibody. Fluorescent images were taken using a confocal laser scanning attachment (MRC1024, BioRad) mounted on an upright microscope (BX50WI, Olympus Corp., Japan) equipped with an 60× water immersion objective (LUMPlanFI, Olympus). Both the anti-NHE1 antibody and the secondary antibody were used after absorbing against PS120 cells. All procedures were performed at room temperature.

Surface Labeling. Cells were incubated with 1 mM NHS-LC-Biotin (Pierce Biotechnology, IL) in PBS containing 0.1 mM $CaCl_2$ and 1 mM $MgCl_2$ for 30 min at room temperature and then solubilized with lysis buffer. The lysate was centrifuged to remove the insoluble fraction. The supernatant was incubated with streptavidin-agarose beads (Pierce) for 1 h at 4 °C, and the beads were then washed five times with lysis buffer. The proteins were eluted with 2× LDS sample buffer by heating and then subjected to immunoblot analysis.

Measurement of ^{22}Na Uptake. $^{22}Na^+$ uptake activity was measured by the K^+/nigericin pH_i clamp method (*19*). Briefly, serum-depleted cells in 24-well plates were preincubated

for 30 min at 37 °C in a Na^+-free choline chloride/KCl medium containing 20 mM HEPES/Tris (pH 7.4), 1.2−140 mM KCl, 2 mM $CaCl_2$, 1 mM $MgCl_2$, 5 mM glucose, and 5 μM nigericin (Invitrogen). $^{22}Na^+$ uptake was started by adding the same choline chloride/KCl solution containing $^{22}NaCl$ (37 kBq/mL: final concentration, 1 mM), 1 mM ouabain, and 0.1 mM bumetanide. In some wells, the uptake solution contained 0.1 mM EIPA. One to 5 min later, cells were rapidly washed four times with ice-cold PBS to terminate $^{22}Na^+$ uptake. pH_i was calculated from $[K^+]_i/[K^+]_o = [H^+]_i/[H^+]_o$ by assuming an intracellular $[K^+]$ of 120 mM. In some experiments, cells were treated with MTS cross-linkers for 15 min at room temperature prior to incubation with pH_i-clamp buffer. The data were normalized on the basis of protein concentration, which was measured using a bicinchoninic assay system (Pierce), using bovine serum albumin as a standard.

Intracellular pH Measurement. Cells were seeded onto 22-mm glass coverslips coated with collagen Type-I (BD Biosciences, NJ). Two days after plating, cells were loaded with 1 μM BCECF/AM (Invitrogen) in a "Na^+ solution" containing 10 mM HEPES/Tris (pH 7.4), 136 mM NaCl, 4 mM KCl, 1.8 mM $CaCl_2$, 1 mM $MgCl_2$, and 5 mM glucose for 10 min at room temperature. The coverslip was mounted on a flow chamber and continuously perfused with solution at 0.6 mL/min by means of a Perista pump (ATTO Corp., Japan). Changes in pH_i were estimated by ratiometric imaging of changes in BCECF fluorescence. Fluorescence was monitored at 510−530 nm by alternatively exciting at 440 and 490 nm through a 505-nm dichroic reflector. Fluorescence images were collected every 5 or 10 s using a cooled CCD camera (ORCA-ER, Hamamatsu photonics K.K., Japan) mounted on an inverted microscope (IX 71, Olympus) with an 20× objective (UApo/340, Olympus) and then were processed with AQUACOSMOS software (Hamamatsu photonics). For NH_4 prepulse, cells were perfused for 5 min with the above Na^+ solution containing 30 mM NH_4Cl, followed by perfusion with a Na^+-free solution (NaCl was replaced by choline Cl). The NHE1-dependent pH_i recovery was induced by reperfusion with the Na^+ solution. The pH_i value was calibrated using a "high K^+ solution" containing 5 μM nigericin adjusted to various pH values. The change in pH_i was also measured by the [^{14}C]benzoic acid-equilibration method (*17*). In this experiment, serum-depleted cells were preincubated for 30 min in bicarbonate-free HEPES-buffered DMEM (pH 7.0) and then incubated in the same medium containing [^{14}C]benzoic acid (1 μCi/mL) for 10 min at 37 °C. After washing four times with ice-cold PBS, the cellular uptake of ^{14}C-radioactivity was measured. The change in pH_i was calculated as described previously (*17*).

RESULTS

Heterodimer Formation between the Wild-Type and Inactive Mutant Exchangers. In this study, we constructed two NHE1 mutants, G309V and E262I (see Figure 1A for their positions in the secondary structure of NHE1). These mutant exchangers showed no EIPA-sensitive $^{22}Na^+$ uptake activity when they were expressed in exchanger-deficient PS120 cells (Figure 1B). Although the fully glycosylated mature form of the wild-type and E262I exchangers were recognized in the immunoblot with anti-NHE1 antibody (Figure 1C), only the immature form of G309V was observed in the immunoblot, suggesting that G309V may be retained in the intracellular membranes. In order to check the surface expression of these mutant exchangers, we carried out the immunofluorescence analysis with anti-NHE1 antibody. Similar to the wild-type NHE1, E262I tagged with HA were expressed at least partly in the plasma membrane, as shown by immunofluorescence observation with anti-HA antibody (Figure 2A; see inset for the fluorescence intensity profile analysis). In contrast, most of G309V proteins were retained in the intracellular membranes (Figure 2A and B for summarized data). Furthermore, G309V proteins were mostly co-stained with the ER marker $DiOC_6(3)$, whereas neither the wild-type nor the E262I exchangers were co-stained (Figure 2C). Thus, the lack of exchange activity of G309V could result from no surface expression of this mutant.

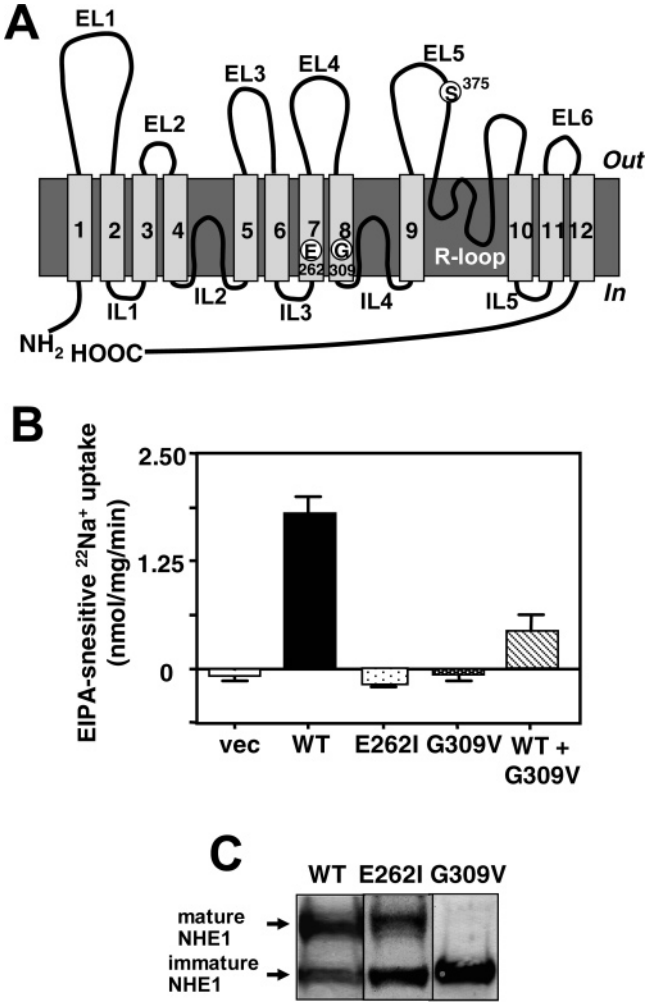

FIGURE 1: Characterization of two inactive mutant exchangers. (A) Secondary structure model of NHE1. The membrane topology has previously been determined by cysteine-accessibility analysis (*18*). Relative positions of mutated residues (Glu^{262}, Gly^{309}, and Ser^{375}) are indicated in the Figure. R-loop, reentrant loop. (B) EIPA-sensitive $^{22}Na^+$-uptake activity in PS120 cells transiently transfected with an empty pECE vector (vec), wild-type NHE1 (WT), E262I, G309V, or wild-type NHE1 plus G309V (0.3 μg for each). Values are the means ± S.D. of triplicate determinations. (C) Immunoblots of proteins obtained from cells stably expressing the wild-type, E262I, or G309V. Cell lysate proteins (50 μg/lane) were applied to 3−8% SDS-PAGE and visualized with anti-NHE1 antibody.

In order to examine whether the G309V mutant interacts with the wild-type NHE1 and thus inhibit its plasma membrane trafficking, we isolated a stable cell line expressing

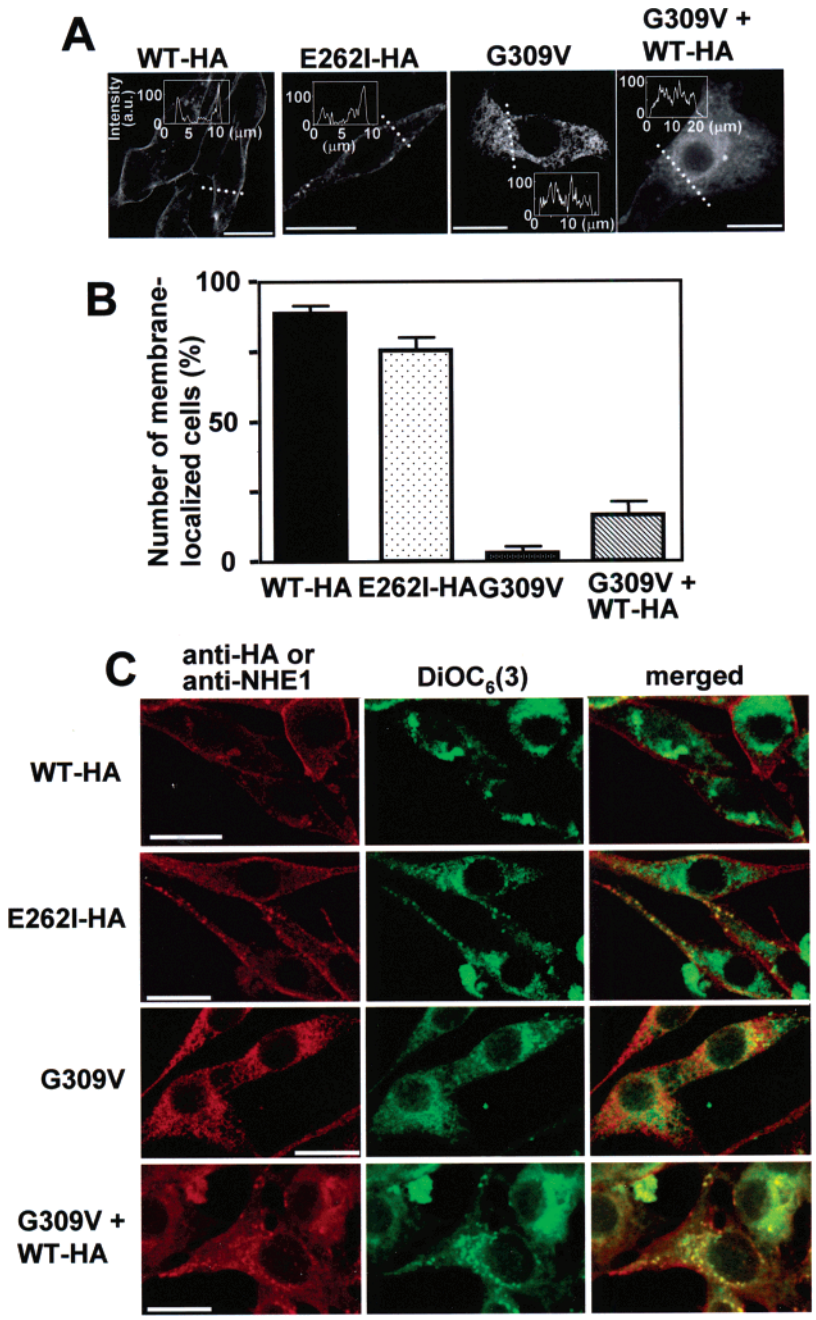

FIGURE 2: Immunofluorescence analysis of two mutant exchangers. (A) Confocal immunofluorescence images of the cells stably expressing the NHE1 variants with or without HA-tag. In one experiment (right panel), cells stably expressing G309V were further transfected with NHE1-HA. Cells were immunostained with anti-HA except for G309V, which were immunostained with anti-NHE1 (third panel). The inset shows the intensity profile of fluorescence along the dotted line. In many cells expressing the wild-type or E262I mutant exchangers, strong fluorescence signals were detected at the cell edge. (B) Summary data for membrane localization of fluorescence signal. The number of cells with a strong fluorescence signal at the cell edge (at least three times more than the average of fluorescence in the internal cell region) was counted. Data are expressed as the mean ± S.D. from six images (total cell number analyzed, 39−101). (C) Double staining of cells for NHE1 and ER maker $DiOC_6$ (*3*). Cells were fixed, permeabilized, and immunostained with anti-HA or anti-NHE1 antibody for G309V (left panels) and then briefly (1 min) incubated with the ER marker $DiOC_6(3)$ (0.1 μM) (middle panels). These fluorescent images were merged (right panels). Scale bars, 20 μm.

G309V and then transfected these cells with HA-tagged wild-type NHE1. In contrast to the predominant localization of the wild-type NHE1 in the plasma membrane upon transfection with a NHE1-carrying vector alone (Figure 2C, left top panel), coexpression of G309V markedly inhibited the surface expression of NHE1 (Figure 2C, left bottom panel and see also Figure 2A and B). Consequently, most of this wild-type NHE1 proteins were retained in the ER, which were co-stained with $DiOC_6(3)$ upon expression of G309V (Figure 2C, right bottom panel). Coexpression also resulted in a strong dominant-negative effect of G309V on exchange activity, as assessed by $^{22}Na^+$ uptake (Figure 1B). Therefore, it is likely that G309V is able to form a heterodimer with the wild-type NHE1 and that dimerization of NHE1 may first occur in the ER membranes, although we do not exclude the possibility that NHE1 subunits interact indirectly.

We next examined whether the wild-type and E262I exchangers exist as a heterodimer in the plasma membrane. We stably coexpressed E262I tagged with an HA epitope (E262I-HA) and the wild-type NHE1 tagged with a Myc

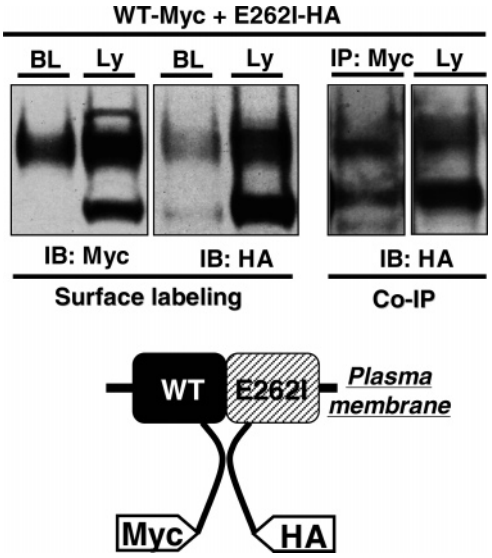

FIGURE 3: Heterodimer formation between the wild-type NHE1 and E262I in the plasma membrane. Cells were stably cotransfected with Myc-tagged NHE1 and HA-tagged E262I and treated with 1 mM NHS-LC-biotin. The biotin-labeled proteins (BL) were collected with streptavidin-agarose beads and analyzed by immunoblotting. Double-transfected cells were also solubilized and subjected to immunoprecipitation with anti-Myc antibody, followed by immunoblotting with anti-HA antibody. The cell lysate was also analyzed by immunoblotting with the indicated antibodies (Ly).

epitope (WT-Myc) in PS120 cells. Cells were surface labeled with NHS-LC-biotin, and biotinylated proteins were recovered with streptavidin-agarose and then analyzed by immunoblotting with anti-HA or anti-Myc antibodies. The results indicate that both proteins were surface-biotinylated (Figure 3), that is, expressed in the plasma membrane. The immature E262I protein band slightly detected in the biotin-treated fraction may be due to the partial membrane permeability of NHS-LC-biotin. To semiquantitatively evaluate the surface expression of NHE1, we estimated the amount of NHE1 proteins adsorbed by streptavidin-agarose beads by subtracting the amount of unbound NHE1 (including immature NHE1) from that of total NHE1 after incubation with beads (data not shown). From such an analysis, we concluded that 45.4 ± 8.7 and 33.3 ± 13.2% (means ± S.D., $n = 3$) of total NHE1 proteins were adsorbed by the beads, that is, expressed in the cell surface for the wild-type and E262I exchangers, respectively. Furthermore, co-immunoprecipitation analysis revealed that E262I-HA was detected in the immunoprecipitates with anti-Myc antibody (Figure 3), suggesting that the Myc-tagged wild-type NHE1 and HA-tagged E262I interact with each other. Hence, surface-labeling and co-immunoprecipitation experiments indicate that wild-type NHE1 forms a heterodimer with E262I in the plasma membrane.

Coexpression of Transport-Deficient NHE1 Mutant Exerts a Dominant-Negative Effect in the Neutral pH_i Range. We next examined the effect of the expression of E262I on the exchange activity of NHE1. We expected that if two active subunits are required for the exchange reaction, heterodimer formation between the wild-type and E262I exchangers would result in the inhibition of activity via the dominant−negative effect of E262I. PS120 cells were transiently transfected with plasmids carrying wild-type NHE1 together with the E262I mutant or an empty vector at a molar ratio of 1:1

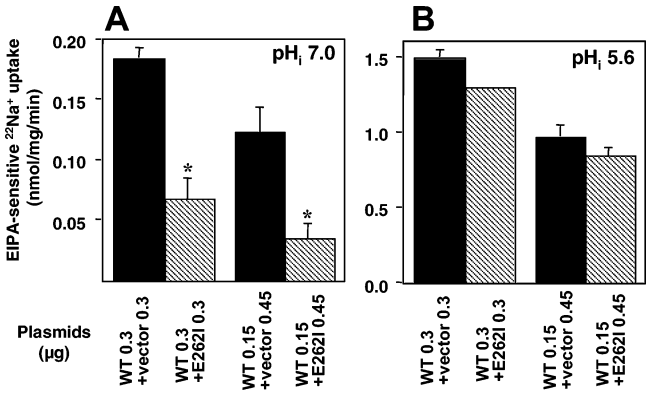

FIGURE 4: Dominant negative effect of E262I on the exchange activity of NHE1. Plasmids carrying the wild-type NHE1 (WT) or E262I were transiently cotransfected into PS120 cells plated on a 24-well plate using Lipofectamine2000. The total quantity of plasmids transfected per well was adjusted to 0.6 μg. In the absence of the E262I plasmid, the total quantity was adjusted with an empty vector. The ratio of the transfected plasmid (WT/E262I or WT/empty vector) was 1:1 and 1:3. Two days after transfection, EIPA-sensitive $^{22}Na^+$ activity was measured at pH_i 7.0 (A) or 5.6 (B) clamped by K^+-nigericin, as described under Experimental Procedures. Values are the means ± S.D. of triplicate determinations. The statistical significance of the data was analyzed by unpaired *t*-test. $^*P < 0.05$.

or 1:3, and exchange activities were assessed by measuring EIPA-sensitive $^{22}Na^+$ uptake at both neutral (7.0) and acidic pH_i (5.6). As shown in Figure 4A, coexpression of E262I resulted in a marked reduction of the activity of the wild-type NHE1 at pH_i 7.0 (more than 50% reduction), that is, E262I exerted the dominant-negative effect. In contrast, expression of E262I had a negligible effect on the exchange activity at acidic pH_i (Figure 4B). These results suggest that heterodimerization with E262I inhibits the transport activity of NHE1 in a pH_i-dependent manner.

We further investigated the dominant-negative effect of E262I under more physiological conditions. To do this, we used CCL39 fibroblastic cells because these cells homogenously express a relatively low amount of endogenous NHE1. The plasmid carrying E262I was cotransfected with DsRed vector carrying a red fluorescent protein as an expression marker. After DsRed fluorescent images were taken, cells were loaded with a fluorescent pH_i indicator, BCECF-AM. Figure 5A shows typical images of DsRed (b) and BCECF fluorescence (c), which were taken in an identical microscopic field. Using this system, the NHE activity was assessed by measuring pH_i recovery after NH_4^+ prepulse. The DsRed-negative cells exhibited a relatively rapid pH_i recovery due to endogenous NHE1 (see cell number 4 in Figure 5A and B). In contrast, the pH_i-recovery rate was dramatically reduced in E262I-expressing DsRed-positive cells (cells numbered 1, 2, and 3). The data from DsRed-positive cells are collected and summarized in Figure 5C and D. While transfection of exogenous wild-type NHE1 accelerated the rate of pH_i recovery, expression of E262I greatly reduced it (Figure 5C and D). Furthermore, expression of E262I shifted the pH_i dependence of the recovery rate to the acidic side (Figure 5E). Figure 5F shows the change in pH_i in response to thrombin. In vector-transfected control CCL39 cells, thrombin induces a rapid cytoplasmic alkalinization via the activation of NHE1, preceded by the transient acidification (asterisk) resulting from Ca^{2+}-

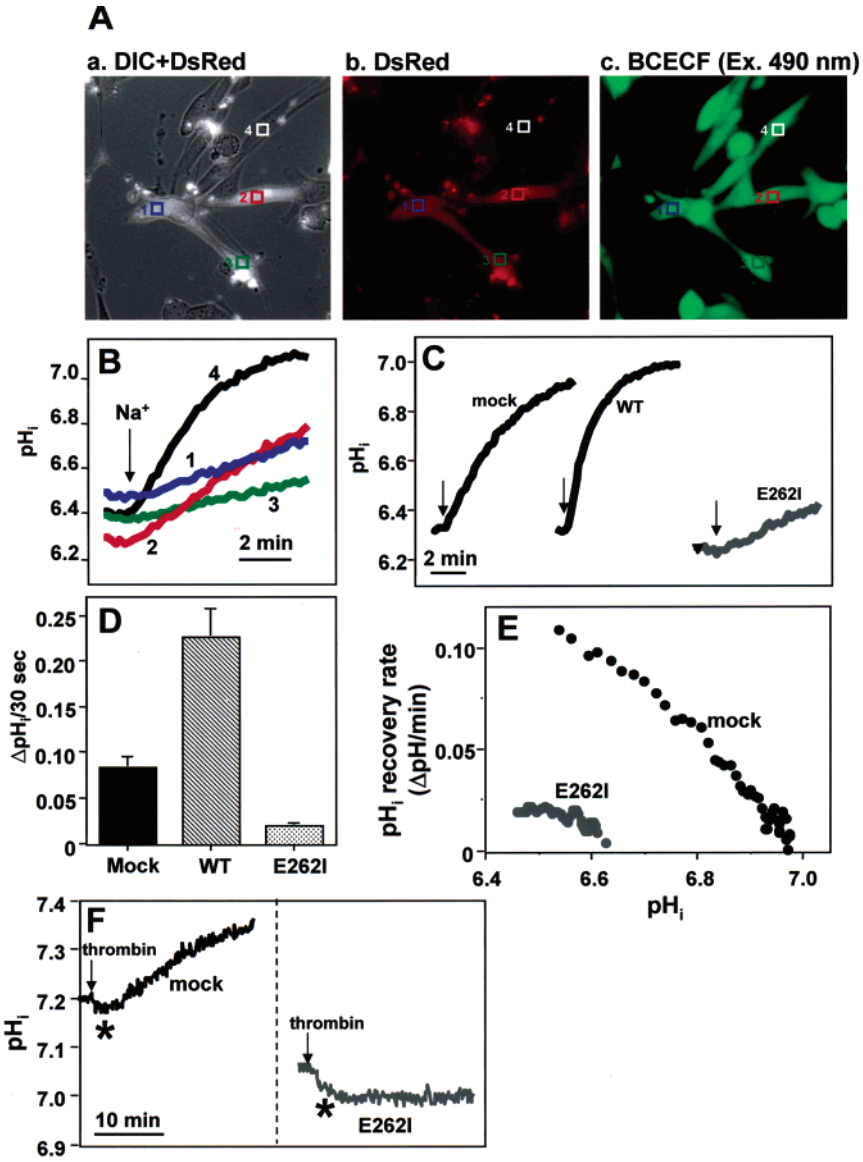

FIGURE 5: Dominant−negative effect of E262I on endogenous NHE1 activity in CCL39 cells. (A) CCL39 cells were grown on collagen-coated glass coverslips and transiently cotransfected with E262I and DsRed (as an expression marker) at a molar ratio of 3:1. Forty-eight hours after transfection, they were serum-depleted for more than 5 h, and a coverslip with a perfusion chamber was mounted on the stage of an inverted microscope fitted with a CCD camera. Differential interference contrast (DIC) and DsRed fluorescence images (a and b) were taken, and then the cells were loaded with 3 μM BCECF-AM for 10 min at room temperature (c, BCECF fluorescence image). (B) pH_i-recovery curves obtained from individually numbered cells. The numbers in B correspond to those in A. Na^+ was added at the time shown by the arrow. (C) and (D) Cells were transiently cotransfected with DsRed together with empty vector (mock), wild-type NHE1, or E262I plasmid, and pH_i-recovery curves were obtained from a DsRed-positive cell. Data were collected from more than 60 DsRed-positive cells in two independent experiments, and a summary of these data is shown. In C, these averaged pH_i-recovery curves are shown, whereas in D, the pH_i increment during 30 s starting from pH_i 6.3 (means ± S.E.) is shown. (E) pH_i dependence of pH_i-recovery rates. The averaged rate of pH_i recovery (C) was calculated from the pH_i increment at every 10 s and plotted against pH_i. (F) Change in pH_i in response to thrombin. CCL39 cells were transiently cotransfected with an empty vector or E262I together with DsRed. At the time indicated by arrows, perfusion was changed to the solution containing 1 uint/mL thrombin. Traces from more than 60 cells were averaged. Asterisks (*) represent the transient acidification resulting from intracellular Ca^{2+} mobilization. These acidifications suggest that cells are capable of undergoing normal cell signaling in response to thrombin.

mobilization (*1*). The expression of E262I completely inhibited this thrombin-induced cytoplasmic alkalinization. Thus, expression of E262I strongly inhibits endogenous NHE1 activity in CCL39 cells in the neutral pH_i range, and thereby abolishes the pH_i regulation in response to growth factors. It should be noted that unlike the $^{22}Na^+$ uptake measurement, we could not assess the exchange activity at very acidic pH_i by measuring pH_i recovery because it was difficult to acidify cells by less than 6.0 by NH_4^+ prepulse.

Na^+/H^+ Exchange Activity Is Inhibited by Symmetrical Intermolecular Cross-Linking at External Cysteine Residues. We expected that if dimerization is essential for the function of NHE1, cross-linking between the two NHE1 subunits would inhibit the Na^+/H^+ exchange reaction by restricting the conformational change of the proteins during transport. We constructed NHE mutants containing a single cysteine using Cys-less NHE1 as a background. Of the 34 single cysteine mutants tested, we found that symmetrical cross-

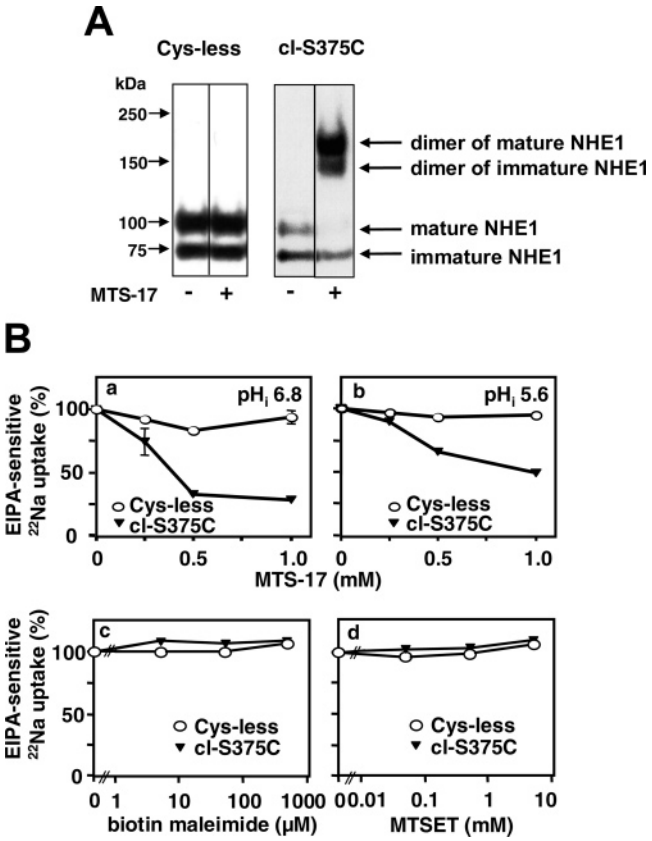

FIGURE 6: Inhibition of NHE1 activity by treatment with cross-linkers. (A) Immunoblot analysis representing the intermolecular cross-linking of cl-S375C proteins. Cells stably expressing Cys-less NHE1 (left panel) or cl-S375C (right panel) were treated with 1 mM MTS-17 for 15 min at 4 °C in BSS and subjected to immunoblot analysis with anti-NHE1 antibody. (B) Cells expressing Cys-less NHE1 or cl-S375C were grown to confluence in 24-well dishes and treated with the indicated concentrations of MTS-17, biotin maleimide, or MTSET for 15 min at room temperature, and the $^{22}Na^+$-uptake activity was measured. In the absence of modifying reagents, EIPA-sensitive $^{22}Na^+$-uptake activity was 10−15 and 40−50 nmol/mg/min at pH$_i$ 6.8 and 5.6 for Cys-less and cl-S375C mutants, respectively. Data were normalized by the values without modifying reagents and represented as means ± S.D. of triplicate determinations. Error bars are sometimes smaller than symbol sizes.

linking occurred with homobifunctional MTS cross-linkers, MTS-2, MTS-6, or MTS-17, at six extracellular sites of NHE1, Pro^{153} in extracellular loop (EL) 2, Asn^{282} and Tyr^{283} in EL4, and Ser^{375}, Thr^{377} and Tyr^{381} in EL5. In this study, we focused on a mutant cl-S375C because a significant reduction of activity was observed upon cross-linking in this mutant. Treatment of the cells with MTS-17 resulted in a mobility shift of cl-S375C from the monomer to the dimer position (right panel of Figure 6A). Immature NHE1 is also cross-linked, as shown by the mobility shift of the lower bands. A similar mobility shift was also observed on treatment with MTS-2 or MTS-6 having shorter spacer arms (data not shown). In contrast to cl-S375C, such a mobility shift was not observed in Cys-less NHE1 (Figure 6A). We investigated whether cross-linking actually affects NHE activity by assessing the effects of cross-linking reagents on EIPA-sensitive $^{22}Na^+$ uptake. Although treatment with MTS-17 had no effect on the activity of Cys-less NHE1, the same treatment markedly suppressed the activity of cl-S375C in a dose-dependent manner both at neutral (6.8) and low pH$_i$ (5.6) (Figure 6B, a and b). Similarly, inhibition of NHE1 activity was also observed as a decrease in the rate of pH$_i$ recovery after acid loading (data not shown). In contrast to MTS-17, the activity was not affected by the monofunctional SH-modifier reagents biotin maleimide or MTSET (Figure 6B, c and d), which have been reported to react with a cysteine residue at position Ser^{375} (*18*), suggesting that inhibition of cl-S375C activity by MTS-17 is not simply due to SH-modification but to intermolecular cross-linking. We did not examine the effects of MTS-2 or MTS-6 on exchange activity because these reagents had a severe toxic effect on cells.

We next investigated several functional properties of cross-linked cl-S375C. As shown in Figure 6B, inhibition of the cl-S375C activity by cross-linking was stronger at high pH$_i$ (75% inhibition at pH$_i$ 6.8) compared to that at low pH$_i$ (50% inhibition at pH$_i$ 5.6). Consistent with this finding, cross-linking with MTS-17 greatly shifted the pH$_i$ dependence of $^{22}Na^+$ uptake to the acidic side and virtually abolished the activity in the neutral pH$_i$ range (Figure 7A), although amino acid substitution of Ser^{375} itself also slightly shifted the pH$_i$ dependence to the acidic side (data not shown). The pH$_i$ dependence of $^{22}Na^+$-uptake activity in Cys-less NHE1 was not affected by treatment with MTS-17 (data not shown). In addition, in cells expressing cl-S375C, cytoplasmic alkalinization in response to thrombin, PMA, or hyperosmotic stress was completely abolished upon treatment with MTS-17 (Figure 7B), whereas significant alkalinization was observed in Cys-less NHE1 (Figure 7B). Lack of NHE1 activation in response to extracellular stimuli is probably due to an acidic shift of the pH$_i$ dependence caused by treatment with MTS-17. In contrast to pH$_i$ regulation, cross-linking with MTS-17 exerted only a small effect on the concentration dependence of extracellular Na^+ (Figure 7C). The K_m values for Na^+ were 8.33 ± 0.64 and 8.95 ± 0.50 mM in Cys-less NHE1 (the trace is not shown) and 12.7 ± 0.7 and 7.99 ± 1.15 mM in cl-S375C in the control and MTS-treated cells, respectively. Treatment with MTS-17 slightly reduced the sensitivity to inhibitor EIPA in cl-S375C (Figure 7D), whereas the same treatment had no effect on EIPA inhibition in Cys-less NHE1 (data not shown). The EIPA concentrations giving half-maximal inhibition (IC$_{50}$) were 78.23 ± 1.56 and 88.1 ± 11.3 nM in Cys-less NHE1 and 126.0 ± 10.3 and 198 ± 10.6 nM in cl-S375C in control and MTS-treated cells, respectively. These results suggest that cross-linking at extracellular sites has a large influence on exchanger function across the membrane, while exerting a moderate effect on the affinities for extracellular Na^+ and EIPA.

DISCUSSION

In this work, we analyzed the functional significance of the dimerization of NHE1 by means of the expression of a dominant-negative mutant exchanger and intermolecular cross-linking. Initially, we showed that the wild-type NHE1 is capable of interacting with surface expression-deficient G309V and with transport-deficient E262I. These observations, together with the data from cross-linking experiment, reinforce the previous findings that NHE1 exists as a dimer in plasma membranes. Experiments with the dominant-negative mutant NHE1 provided evidence that two active subunits are required for the function of NHE1. The expres-

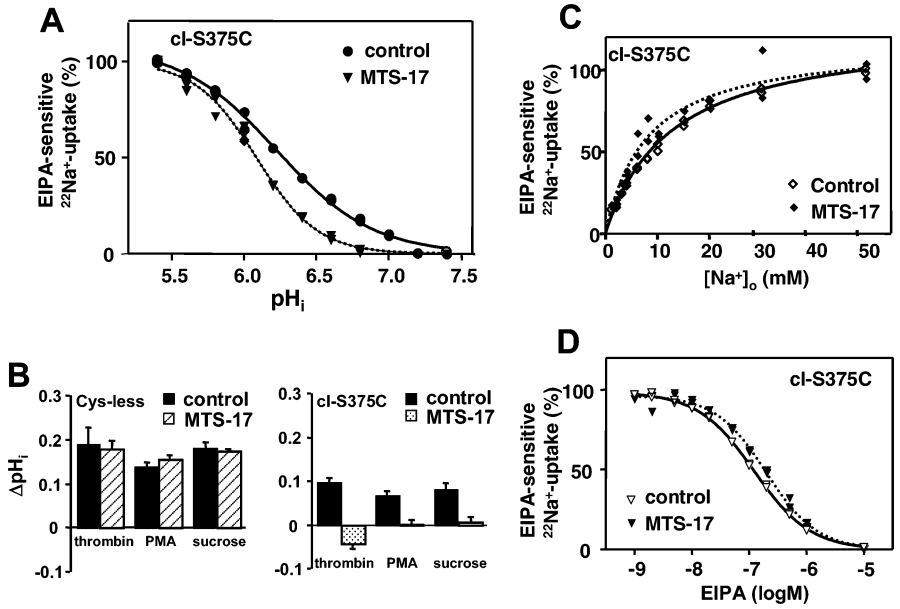

FIGURE 7: Functional properties of cl-S375C after cross-linker treatment. (A) pH_i dependence of EIPA-sensitive $^{22}Na^+$-uptake activity measured in cells expressing cl-S375C treated with or without MTS-17. The $^{22}Na^+$ uptake at pH_i 5.4 was reduced after cross-linker treatment (Figure 6B). Data were normalized to those at pH_i 5.4. (B) Change in pH_i in response to various external stimuli. Cells expressing Cys-less NHE1 or cl-S375C were incubated with or without 250 μM MTS-17 for 15 min at room temperature, and then the external stimuli-induced change in pH_i was measured using the [^{14}C]benzoic acid-equilibration method as described in Experimental Procedures. Cells were stimulated with 1 unit/mL thrombin, 1 μM PMA, or 200 mM sucrose (hyperosmotic stress). (C) and (D) Effect of MTS-17 on the concentration dependences of EIPA-sensitive $^{22}Na^+$ uptake on external Na^+ ($[Na^+]_o$) and EIPA in cells expressing cl-S375C. Cells were treated with 500 μM MTS-17 for 15 min at room temperature and pH_i-clamped at 5.6, and then the $^{22}Na^+$ uptake was measured in the presence of various concentrations of Na^+ (C) or EIPA (D). Data were normalized by the values at 50 mM Na^+ for C or at 1 nM EIPA for D.

sion of transport-deficient E262I in CCL39 cells dramatically reduced the exchange activity of endogenous NHE1 through an acidic shift in the pH_i dependence of exchange activity (Figure 5). In addition, coexpression of E262I, together with wild-type NHE1, markedly reduced exchange activity at neutral pH_i, whereas it exerted only a marginal effect on the activity at acidic pH_i (Figure 4). These data suggest that heterodimer formation between the wild-type protein and the E262I mutant exchanger results in a marked inhibition of exchange activity by inducing an acidic shift of the pH_i dependence, suggesting that dimerization would be essential for physiological exchange activity.

Secondary active transporters such as NHE1 are generally thought to have two major alternating conformations during the transport cycle, outward- and inward-facing orientations. This is also compatible with the recently solved crystal structures of two major facilitator superfamily transporters, the glycerol-3-phosphate transporter (*20*) and the lactose permease of *E. coli* (*21*). In the E262I subunit of the NHE1 heterodimer, such a conformational change may not be able to take place because this subunit is transport-deficient. Therefore, it is possible that the fixed structure of E262I restricts the free motion of a neighboring active subunit. Intermolecular cross-linking would provide another approach to restrict such motion between subunits. The treatment of cells expressing cl-S375C with MTS-17 markedly reduced exchange activity. Importantly, this inhibition mainly occurs by shifting the pH_i dependence of exchange to the acidic side and partly by decreasing the maximal activity at acidic pH_i (V_{max}) and consequently abolished extracellular stimuli-induced cytoplasmic alkalinization. The same treatment, however, did not exert a large influence on the apparent affinities for extracellular Na^+ or the inhibitor EIPA. Intermolecular cross-linking at position Ser^{375}, which is located in EL5, occurred upon treatment with all tested MTS reagents. These reagents have different spacer arms (MTS-2, 5.2 Å; MTS-6, 10.4 Å; and MTS-17, 24.7 Å), suggesting that Ser^{375} in EL5 is mobile over a relatively long distance at least between 5 and 25 Å. In membrane transporters, the movement of extracellular loops often plays an important role in the transport cycle. For example, in the glycine transporter GLYT2, the first extracellular loop is reported to alter its accessibility to SH-modification reagents during the transport cycle (*22*). Our data suggest that cross-linking at position Ser^{375} would restrict the motion of EL5 to less than 25 Å between NHE1 subunits and in turn lead to a marked reduction in exchange activity. These results can be explained if it is assumed that dimerization is essential for NHE1 function and that the two NHE1 subunits undergo conformational changes in a concerted manner. Cross-linking would restrict the coupled motion between the subunits, thereby leading to the inhibition of exchange activity possibly by an apparent reduction in pH_i sensitivity. Thus, the data obtained from two different approaches, the dominant-negative experiment and cross-linking, overall suggest that the exchange activity depends on a coupled conformational change of two subunits at physiological pH_i and raise the interesting possibility that the pH-sensing machinery of NHE1 may be fully functional only when two subunits are active. This idea is consistent with previous reports (*12*−*14*) suggesting that subunit-subunit interaction may be important for the function of the exchanger. For example, the Na^+/H^+ exchange in kidney brush border membrane vesicles was reported to exhibit the sigmoidal Na^+ dependence under certain conditions (*12*, *13*). Also, the pH_i dependence of exchange activity was recently reported to be best explained by allosteric kinetics on the basis of the assumption of a dimeric transporter (*14*).

It is of interest to note that inhibition of activity by expression of E262I was not detected at low pH_i (Figure 4), suggesting that the wild-type NHE1 subunit of the heterodimer is functional when intracellular H^+ concentration is sufficiently high. This is consistent with a previous report demonstrating that the dominant-negative effect of E262I on Na^+/H^+ exchange activity was not detected in measurements taken at acidic pH_i (*9*). This observation may be explained if we assume that E262I affects H^+-regulatory sites but not ion-transport sites of the neighboring active subunit. At present, there is substantial evidence that the ion transport machinery is located within the membrane-spanning region. For example, previous studies have shown that mutations of residues within TM4 and TM9 of NHE1 reduce the affinity for Na^+ or the cation transport activity (*23*−*27*). Furthermore, crystal structure determination and mutational studies on the bacterial Na^+/H^+ antiporter NhaA suggest that the ion binding site consists of several polar residues within the transmembrane helices (*28*, *29*). A high-resolution crystal structure of a bacterial Na^+/Cl^--dependent neurotransmitter transporter homologue provided more direct proof that residues within the transmembrane helices coordinate two Na^+ ions (*30*). Thus, it is reasonable to suppose that each subunit of NHE1 has an ion transport pathway and the active subunit of the heterodimer is capable of catalyzing the transport reaction under particular conditions. However, previous biochemical data (*6*, *8*) suggest that the H^+-regulatory sites and ion-transport sites of exchangers are a part of different structural elements and that the acidic shift in the pH_i dependence of exchange mainly results from decrease in the H^+ affinity at regulatory sites. Recent crystal structure determination of NhaA (*28*) and the subsequent electrostatic analysis (*31*) predicted that charged residues with unusual pK_a values, as the pH-sensor, may undergo protonation/deprotonation reactions and subsequently induce the overall conformational changes resulting in the formation of the active form. In the case of NHE1, we have previously identified crucial elements regulating pH sensing: (i) Arg^{440} in IL5 (*32*), (ii) a juxtamembrane cytoplasmic domain (aa 503−595) (*19*), and (iii) a calcineurin B homologous protein (CHP) interacting with a part of this juxtamembrane domain (*33*, *34*). Arg^{327} in IL4 has also recently been reported to be an important residue for determining H^+ affinity (*14*). Interaction with E262I may possibly modify these regions of the neighboring active subunit. Intermolecular cross-linking at position Ser^{375} may also exert similar effects on H^+-regulatory sites. This led us to predict that these important regions of NHE1 may exist close to the interface between subunits. We recently reported that deletion of the putative juxtamembrane dimer-interface region (aa 560−580) markedly decreased the pH_i-sensitivity of NHE1 (*11*).

The functional significance of oligomerization has only been studied for a few transporters. Some experimental data (*35*−*38*) suggest that NhaA exists as a dimer in membranes and that the subunits may functionally interact. A recent study using a fluorescence resonance energy transfer technique (*38*) suggested that the *Helicobacter pylori* Na^+/H^+ antiporter NhaA monomers exerts conformational change during transport. Furthermore, the transport-deficient mutant form of *Saccaromyces cerevisiae* Na^+/H^+ antiporter Nha1p was reported to exert the dominant-negative effect upon coexpression with the wild-type Nha1p (*39*). These studies suggest the functional importance for dimerization of bacteria and yeast Na^+/H^+ antiporters. The glucose transporter GLUT1 (*40*) and the serotonin transporter SERT (*41*) have also been suggested to function as homo-oligomers, whereas the bacterial lactose permease LacY (*42*) and the renal type IIa Na^+/phosphate cotransporter (*43*) have been shown to function as monomers. However, in the case of NHE1, the functional consequence of dimerization appears to be more complex, that is, dimerization is necessary for NHE1 to function in the physiological pH_i range, although each subunit is capable of functioning at a more acidic pH_i. In this context, it is of interest to note that the lactose transport protein LacS from *Streptococcus thermophilus* was recently shown to be a cooperative dimer in which two subunits are functionally coupled in ΔH^+-driven substrate symport, whereas the monomer is sufficient for substrate/substrate exchange (*44*).

In summary, we presented evidence that dimerization may be essential for NHE1 to exert exchange activity in neutral pH_i range. We predict that two active NHE1 subunits would be required for NHE1 to possess the physiologically relevant H^+ affinity presumably at the H^+-regulatory sites. Although the underlying molecular mechanism is still unknown, our present findings provide good evidence for the functional importance of the dimerization of NHE1.

ACKNOWLEDGMENT

We thank Dr. M. Shigekawa for fruitful discussions and Mrs. M. Nakatani (Ms. M. Ookubo) for technical assistance.

REFERENCES

1. Wakabayashi, S., Shigekawa, M., and Pouyssegur, J. (1997) Molecular physiology of vertebrate Na^+/H^+ exchangers, *Physiol. Rev. 77*, 51−74.
2. Orlowski, J., and Grinstein, S. (2004) Diversity of the mammalian sodium/proton exchanger SLC9 gene family, *Pflugers Arch. 447*, 549−565.
3. Counillon, L., and Pouyssegur, J. (2000) The expanding family of eucaryotic Na^+/H^+ exchangers, *J. Biol. Chem. 275*, 1−4.
4. Putney, L. K., Denker, S. P., and Barber, D. L. (2002) The changing face of the Na^+/H^+ exchanger, NHE1: structure, regulation, and cellular actions, *Annu. Rev. Pharmacol. Toxicol. 42*, 527−552.
5. Slepkov, E., and Fliegel, L. (2002) Structure and function of the NHE1 isoform of the Na^+/H^+ exchanger, *Biochem. Cell Biol. 80*, 499−508.
6. Aronson, P. S., Nee, J., and Suhm, M. A. (1982) Modifier role of internal H^+ in activating the Na^+-H^+ exchanger in renal microvillus membrane vesicles, *Nature 299*, 161−163.
7. Aronson, P. S. (1985) Kinetic properties of the plasma membrane Na^+-H^+ exchanger, *Annu. Rev. Physiol. 47*, 545−560.
8. Wakabayashi, S., Hisamitsu, T., Pang, T., and Shigekawa, M. (2003) Kinetic dissection of two distinct proton binding sites in Na^+/H^+ exchangers by measurement of reverse mode reaction, *J. Biol. Chem. 278*, 43580−43585.
9. Fafournoux, P., Noel, J., and Pouyssegur, J. (1994) Evidence that Na^+/H^+ exchanger isoforms NHE1 and NHE3 exist as stable dimers in membranes with a high degree of specificity for homodimers, *J. Biol. Chem. 269*, 2589−2596.
10. Fliegel, L., Haworth, R. S., and Dyck, J. R. (1993) Characterization of the placental brush border membrane Na^+/H^+ exchanger: identification of thiol-dependent transitions in apparent molecular size, *Biochem. J. 289*, 101−107.
11. Hisamitsu, T., Pang, T., Shigekawa, M., and Wakabayashi, S. (2004) Dimeric interaction between the cytoplasmic domains of the Na^+/H^+ exchanger NHE1 revealed by symmetrical intermolecular cross-linking and selective co-immunoprecipitation, *Biochemistry 43*, 11135−11143.

12. Otsu, K., Kinsella, J., Sacktor, B., and Froehlich, J. P. (1989) Transient state kinetic evidence for an oligomer in the mechanism of Na^+-H^+ exchange, *Proc. Natl. Acad. Sci. U.S.A. 86*, 4818−4822.
13. Otsu, K., Kinsella, J. L., Koh, E., and Froehlich, J. P. (1992) Proton dependence of the partial reactions of the sodium-proton exchanger in renal brush border membranes, *J. Biol. Chem. 267*, 8089−8096.
14. Lacroix, J., Poet, M., Maehrel, C., and Counillon, L. (2004) A mechanism for the activation of the Na/H exchanger NHE-1 by cytoplasmic acidification and mitogens, *EMBO Rep. 5*, 91−96.
15. Bertrand, B., Wakabayashi, S., Ikeda, T., Pouyssegur, J., and Shigekawa, M. (1994) The Na^+/H^+ exchanger isoform 1 (NHE1) is a novel member of the calmodulin-binding proteins. Identification and characterization of calmodulin-binding sites, *J. Biol. Chem. 269*, 13703−13709.
16. Pouyssegur, J., Sardet, C., Franchi, A., L'Allemain, G., and Paris, S. (1984) A specific mutation abolishing Na^+/H^+ antiport activity in hamster fibroblasts precludes growth at neutral and acidic pH, *Proc. Natl. Acad. Sci. U.S.A. 81*, 4833−4837.
17. Wakabayashi, S., Fafournoux, P., Sardet, C., and Pouyssegur, J. (1992) The Na^+/H^+ antiporter cytoplasmic domain mediates growth factor signals and controls "H^+-sensing", *Proc. Natl. Acad. Sci. U.S.A. 89*, 2424−2428.
18. Wakabayashi, S., Pang, T., Su, X., and Shigekawa, M. (2000) A novel topology model of the human Na^+/H^+ exchanger isoform 1, *J. Biol. Chem. 275*, 7942−7949.
19. Ikeda, T., Schmitt, B., Pouyssegur, J., Wakabayashi, S., and Shigekawa, M. (1997) Identification of cytoplasmic subdomains that control pH-sensing of the Na^+/H^+ exchanger (NHE1): pH-maintenance, ATP-sensitive, and flexible loop domains, *J. Biochem. (Tokyo) 121*, 295−303.
20. Huang, Y., Lemieux, M. J., Song, J., Auer, M., and Wang, D. N. (2003) Structure and mechanism of the glycerol-3-phosphate transporter from Escherichia coli, *Science 301*, 616−620.
21. Abramson, J., Smirnova, I., Kasho, V., Verner, G., Kaback, H. R., and Iwata, S. (2003) Structure and mechanism of the lactose permease of Escherichia coli, *Science 301*, 610−615.
22. Lopez-Corcuera, B., Nunez, E., Martinez-Maza, R., Geerlings, A., and Aragon, C. (2001) Substrate-induced conformational changes of extracellular loop 1 in the glycine transporter GLYT2, *J. Biol. Chem. 276*, 43463−43470.
23. Counillon, L., Franchi, A., and Pouyssegur, J. (1993) A point mutation of the Na^+/H^+ exchanger gene (NHE1) and amplification of the mutated allele confer amiloride resistance upon chronic acidosis, *Proc. Natl. Acad. Sci. U.S.A. 90*, 4508−4512.
24. Counillon, L., Noel, J., Reithmeier, R. A., and Pouyssegur, J. (1997) Random mutagenesis reveals a novel site involved in inhibitor interaction within the fourth transmembrane segment of the Na^+/H^+ exchanger-1, *Biochemistry 36*, 2951−2959.
25. Slepkov, E. R., Chow, S., Lemieux, M. J., and Fliegel, L. (2004) Proline residues in transmembrane segment IV are critical for activity, expression and targeting of the Na^+/H^+ exchanger isoform 1, *Biochem. J. 379*, 31−38.
26. Noel, J., Germain, D., and Vadnais, J. (2003) Glutamate 346 of human Na^+-H^+ exchanger NHE1 is crucial for modulating both the affinity for Na^+ and the interaction with amiloride derivatives, *Biochemistry 42*, 15361−15368.
27. Khadilkar, A., Iannuzzi, P., and Orlowski, J. (2001) Identification of sites in the second exomembrane loop and ninth transmembrane helix of the mammalian Na^+/H^+ exchanger important for drug recognition and cation translocation, *J. Biol. Chem. 276*, 43792−43800.
28. Hunte, C., Screpanti, E., Venturi, M., Rimon, A., Padan, E., and Michel, H. (2005) Structure of a Na^+/H^+ antiporter and insights into mechanism of action and regulation by pH, *Nature 435*, 1197−1202.
29. Inoue, H., Noumi, T., Tsuchiya, T., and Kanazawa, H. (1995) Essential aspartic acid residues, Asp-133, Asp-163 and Asp-164, in the transmembrane helices of a Na^+/H^+ antiporter (NhaA) from Escherichia coli, *FEBS Lett. 363*, 264−268.
30. Yamashita, A., Singh, S. K., Kawate, T., Jin, Y., and Gouaux, E. (2005) Crystal structure of a bacterial homologue of Na^+/Cl^--dependent neurotransmitter transporters, *Nature 437*, 215−223.
31. Olkhova, E., Hunte, C., Screpanti, E., Padan, E., and Michel, H. (2006) Multiconformation continuum electrostatics analysis of the NhaA Na^+/H^+ antiporter of Escherichia coli with functional implications, *Proc. Natl. Acad. Sci. U.S.A. 103*, 2629−2634.
32. Wakabayashi, S., Hisamitsu, T., Pang, T., and Shigekawa, M. (2003) Mutations of Arg440 and Gly455/Gly456 oppositely change pH sensing of Na^+/H^+ exchanger 1, *J. Biol. Chem. 278*, 11828−11835.
33. Pang, T., Hisamitsu, T., Mori, H., Shigekawa, M., and Wakabayashi, S. (2004) Role of calcineurin B homologous protein in pH regulation by the Na^+/H^+ exchanger 1: tightly bound Ca^{2+} ions as important structural elements, *Biochemistry 43*, 3628−3636.
34. Pang, T., Su, X., Wakabayashi, S., and Shigekawa, M. (2001) Calcineurin homologous protein as an essential cofactor for Na^+/H^+ exchangers, *J. Biol. Chem. 276*, 17367−17372.
35. Williams, K. A., Geldmacher-Kaufer, U., Padan, E., Schuldiner, S., and Kuhlbrandt, W. (1999) Projection structure of NhaA, a secondary transporter from Escherichia coli, at 4.0 A resolution, *EMBO J. 18*, 3558−3563.
36. Williams, K. A. (2000) Three-dimensional structure of the ion-coupled transport protein NhaA, *Nature 403*, 112−115.
37. Gerchman, Y., Rimon, A., Venturi, M., and Padan, E. (2001) Oligomerization of NhaA, the Na^+/H^+ antiporter of Escherichia coli in the membrane and its functional and structural consequences, *Biochemistry 40*, 3403−3412.
38. Karasawa, A., Tsuboi, Y., Inoue, H., Kinoshita, R., Nakamura, N., and Kanazawa, H. (2005) Detection of oligomerization and conformational changes in the Na^+/H^+ antiporter from Helicobacter pylori by fluorescence resonance energy transfer, *J. Biol. Chem. 280*, 41900−41911.
39. Mitsui, K., Yasui, H., Nakamura, N., and Kanazawa, H. (2005) Oligomerization of the Saccharomyces cerevisiae Na^+/H^+ antiporter Nha1p: implications for its antiporter activity, *Biochim. Biophys. Acta. 1720*, 125−136.
40. Zottola, R. J., Cloherty, E. K., Coderre, P. E., Hansen, A., Hebert, D. N., and Carruthers, A. (1995) Glucose transporter function is controlled by transporter oligomeric structure. A single, intramolecular disulfide promotes GLUT1 tetramerization, *Biochemistry 34*, 9734−9747.
41. Kilic, F., and Rudnick, G. (2000) Oligomerization of serotonin transporter and its functional consequences, *Proc. Natl. Acad. Sci. U.S.A. 97*, 3106−3111.
42. Sahin-Toth, M., Lawrence, M. C., and Kaback, H. R. (1994) Properties of permease dimer, a fusion protein containing two lactose permease molecules from Escherichia coli, *Proc. Natl. Acad. Sci. U.S.A. 91*, 5421−5425.
43. Kohler, K., Forster, I. C., Lambert, G., Biber, J., and Murer, H. (2000) The functional unit of the renal type IIa Na^+/Pi cotransporter is a monomer, *J. Biol. Chem. 275*, 26113−26120.
44. Veenhoff, L. M., Heuberger, E. H., and Poolman, B. (2001) The lactose transport protein is a cooperative dimer with two sugar translocation pathways, *EMBO J. 20*, 3056−3062.

BI0608616